Automatic travelling of agricultural support robot for a fruit farm - Verification of effectiveness of real-time kinematic-global navigation satellite system and developed a simulator for specification design

Ren Hiraoka,[1] Yuya Aoyagi,[2,3] Kazuki Kobayashi[4]

[1]Faculty of Engineering, Shinshu University, Nagano city, Nagano Pref.; [2]Research Centre for Social Systems, Shinshu University, Nagano city, Nagano Pref.; [3]Faculty of Agriculture, University of the Ryukyus, Nakagami-gun, Okinawa Pref.; [4]Academic Assembly, Shinshu University, Nagano city, Nagano Pref., Japan

Abstract

Labour shortages and fatal accidents in agricultural work have recently emerged as critical problems in Japan, necessitating productivity enhancement, workload reduction, and safety assurance. Therefore, in Japan and countries with similar agricultural environments, the use of small and inexpensive agricultural robots that can be employed in mountain farms and orchards is desirable. In this study, a dynamic positioning test was performed in orchards in a mountainous region to verify the positioning accuracy and stability of the global navigation satellite system (GNSS) and real-time kinematic (RTK)-GNSS. In addition, a simulator for an agricultural robot that could consider the environmental information of orchards was developed, and driving tests were conducted using the GNSS data acquired in the simulation. The error of the GNSS module was set to be higher than that for the measured value, and the robot travelling in the orchard was simulated. The results of GNSS positioning tests in an orchard near a mountainous area indicate that in the specific environmental conditions, the RTK-GNSS and stand-alone (SA)-GNSS can attain a positioning accuracy with an order of tens of centimetres and few metres, respectively. Moreover, the simulation results based on the GNSS positioning results indicate that a vehicle implementing RTK-GNSS and a simple obstacle detection sensor can travel autonomously in a farmyard without colliding with the tree rows. In contrast, a vehicle implementing SA-GNSS and a simple obstacle detection sensor cannot drive autonomously in an orchard and must realise self-positioning using a more accurate sensor. Therefore, the proposed approach of realising simulations of autonomous agricultural robots based on GNSS data from a real orchard can facilitate the evaluation of practical agricultural robots and confirm safe travelling roots. Furthermore, the results demonstrate the possibility of developing small agricultural robots for orchards. We conducted the GNSS positioning test in an orchard at an altitude of approximately 830 m. A similar performance can be expected under alike agricultural situations because the error of the GNSS module was set to be higher than the measured value in the driving simulation test.

Introduction

Recently, the declining and ageing population of agricultural workers in Japan has emerged as a critical problem. The agricultural working population (the number of people engaged in self-employed farming as a profession) has decreased from approximately 1.757 million (2015) to approximately 1.363 million (2020) in the last five years. Moreover, the proportion of individuals aged 65 y or more in the agricultural working population has increased from approximately 64.9% (2015) to approximately 69.6% (2020) (Japan Ministry of Agriculture, Forestry and Fisheries, 2021). The agricultural industry generally involves a considerable workload with high accident risks. Notably, the fatal injury rate per 100,000 farmers was evaluated to be as high as 16.7% (2019), higher than that in other industries (National Agriculture and Food Research Organization, 2019).

Consequently, enhancing productivity, reducing the labour load, and ensuring safety is necessary. The Japan Ministry of Agriculture, Forestry and Fisheries (2020) recommends using smart agricultural technology in various areas, such as mountainous regions, for entities such as vegetables and fruit trees. In other words, automated machine work is significant to enhance safety and efficiency to overcome the abovementioned problems.

To ensure efficient robotic operations in the agricultural domain, locating the work area and ensuring the robot self-posi-

tioning is necessary. In this context, the global navigation satellite system (GNSS) technology has been widely implemented (Weise *et al.*, 2000; Keicher and Seufert, 2000; Nørremark *et al.*, 2008; Kayacan *et al.*, 2014; Allred *et al.*, 2018; Freeland *et al.*, 2019) to enable the development of cost-effective agricultural robots (Søgaard and Lund, 2007; Hossein, 2013; Rovira-Más *et al.*, 2015). Moreover, expensive and highly accurate systems such as real-time kinematic (RTK)-GNSS have been implemented to automate large agricultural machines. For example, in Japan, research and development of robotic farm machinery based on high-precision GNSS have been conducted for paddy rice production machinery such as tractors, rice transplanters, and combine harvesters (Nagasaka *et al.*, 2000; Kise *et al.*, 2002; Matsuo *et al.*, 2009; Iida *et al.*, 2013; Zhang *et al.*, 2015; Ogura, 2017; Miyamoto *et al.*, 2017), and large machinery has been distributed commercially. However, it is economically infeasible to incorporate expensive positioning systems in small-scale agricultural machinery in relatively small fields. Consequently, researchers actively seek techniques to attain high accuracy at a low cost (Chosa *et al.*, 2007; Barawid and Noguchi, 2008; Barawid and Noguchi, 2010). Recently, low-cost RTK-GNSS systems were introduced in agricultural machinery (Kaizu *et al.*, 2018; Han *et al.*, 2019).

Notably, not all precision agriculture operations require the same level of location accuracy (Pérez-Ruiz *et al.*, 2021). Nevertheless, the accuracy should be satisfactory in the operational environment. Even in highly accurate systems such as RTK-GNSS, the accuracy decreases as the distance from the base station increases (Alkan *et al.*, 2020), and it is necessary to verify the accuracy in different countries and regions in terms of the number of satellite signals available. Some researchers attempted to validate the GNSS accuracy in agricultural areas in different areas worldwide (Pérez-Ruiz *et al.*, 2011; Guo *et al.*, 2018; Catania *et al.*, 2020). In an open-sky environment such as a paddy rice field, the GNSS can help realise highly accurate positioning (Santos *et al.*, 2019).

In contrast, in an orchard or mountainous areas, the presence of trees affects the GNSS positioning accuracy. In particular, Li *et al.* (2009) stated that robot localisation based on GNSS receivers is susceptible to operation failure when trees or leaves block the GNSS signals. Furthermore, Kabir *et al.* (2016) indicated that the root mean square error (RMSE) values pertaining to the use of a multi-GNSS receiver in an open field, an orchard, and a mountainous area in Korea were 0.152 m, 0.182 m, and 1.13 m, respectively. Pini *et al.* (2020) indicated that the RTK-GNSS positioning errors (approximately 2.5-10 cm) under foliage in an orchard or vineyard were higher than those in the open-sky condition. Thus, a GNSS system cannot yield sufficient accuracy for robotic work in orchards and mountainous agricultural areas.

The feasibility of combinations of different methods has been examined to achieve robust and accurate positioning in orchards or mountain areas. In addition to GNSS systems, vision cameras, and light detection and ranging (LiDAR) frameworks can be used as local sensors to sense environmental information, and filter processing and simultaneous localisation and mapping (SLAM) can be conducted to estimate the self-position with high accuracy (Cheein *et al.*, 2011; Blok *et al.*, 2019; Guevara *et al.*, 2020). However, applying methods such as LiDAR and SLAM requires high-precision sensors and powerful computing resources, which renders the implementation expensive. In addition, the latter consumes much power, which reduces the battery life. Although the benefits of such implementations may offset the installation cost in the case of large-scale and highly efficient machines, the economic feasibility is questionable in the case of small farm machines.

In Japan, mountainous areas account for approximately 40% of the total arable land, and the average area per farm entity is 2.2 ha in prefectures excluding Hokkaido (Japan Ministry of Agriculture, Forestry and Fisheries, 2021). These small-scale farmers usually use small and medium-sized machines to achieve reasonable safety and workability under environmental conditions specific to mountainous areas and Japanese orchards. In this context, the use of small and inexpensive agricultural robots that can be used in mountain farms and orchards is desirable. Therefore, in this study, we focused on small robots for transporting harvested production (heavy goods) in mountain orchards. It is necessary to measure the accuracy of GNSS in Japanese mountain orchards and evaluate the applicability of using GNSS for robotic work in such environments. In addition, combinations of various sensors must be tested to develop a low-cost and practical robot while minimising the number of necessary sensors. Simulations based on real GNSS data and environmental information can help validate practical robotic tasks and determine the appropriate robot specifications.

Research on small robots in orchards in mountainous areas is insufficient to develop practical robots. In this study, a dynamic positioning test was conducted in orchards in a mountainous region to verify the positioning accuracy and robustness of SA-GNSS and low-cost RTK-GNSS. In addition, a simulator for an agricultural robot was developed considering the environmental information of orchards, and driving tests were conducted using GNSS data acquired in the simulation. Finally, the results were analysed to clarify the effectiveness of GNSS for robotic operations in Japanese fruit orchards and the importance of evaluating practical robot travelling *via* simulations.

The remaining paper is organised as follows. The next section describes the conditions associated with the dynamic GNSS positioning experiments. Moreover, details of the developed simulator for an autonomous agricultural robot are presented, and the driving tests performed considering the acquired GNSS data and environmental information are described. The following one presents the results of GNSS positioning in orchards and simulated driving tests. The effectiveness of GNSS in Japanese orchards and simulation methods to determine the practical specifications of the autonomous agricultural robot are discussed. Finally, the last section presents the concluding remarks.

Materials and Methods

Survey of real-time kinematic-global navigation satellite system receiving status in fruit farms

The experiment of this study was conducted on 18th September 2020 at a fruit orchard in Minowa-machi, Kamiina-gun, Nagano Prefecture, Japan, which is located near the foothill of the eastern side of Kurosawayama Mountain (2126 m above sea level) and the north-eastern side of Mt. Kyoga (2296 m above sea level). The altitude of the orchard is approximately 830 m. The prefectural governor designates the area in which the orchard is located as being unfavourable owing to its natural, economic, and social conditions and being covered by the direct payment scheme for mountainous areas in April 2020 (Nagano Prefecture, 2020).

A dual-frequency RTK-GNSS receiver and a single-frequency SA-GNSS receiver were used in the experiment of this study. The former cost was approximately 450 US dollars, and the correction signal was provided by a commercial service (SoftBank Corp., Ichimill). The RTK correction signal was transmitted from more

than 3300 base stations nationwide and was valid within the softbank long term evolution (LTE) area. The position output rate of the RTK-GNSS receiver was 1 Hz. Table 1 lists the specifications of the RTK-GNSS receiver and SA-GNSS receiver. The accuracy of the GNSS receivers in the field was verified from the position information acquired by carrying the receiver on a cart along the same route. Based on a previous report, the location information was calculated from the acquired latitude and longitude (Kawase, 2011).

To perform a comparative analysis, the results of three types of fields were considered: a short-tree apple field, a new type of apple field (high-density planting and short tree), and a pear field. Figure 1 shows the images of the harvesting route in each field. The centre of a harvest aisle was used as the experimental route. A starting point, intermediate points, and an endpoint were set on each route, and the distance between each pair of points was measured using a measuring tape (UniGrip Flix 50 m). The operator pushed the cart at a normal walking speed (approximately 0.5-1.0 ms^{-1}) and stopped it at each point of the route for approximately 30-60 s.

In the verification process, we compared the measured distance with the calculated distance based on the information from both receivers. Table 2 lists the experimental conditions in each orchard. In addition, we examined the positioning status of all the roads in the field (to examine if any difficulties were encountered in positioning) and compared the accuracy of both receivers. Finally, the results were analysed to clarify the effectiveness of GNSS in the fruit orchard in Japan in a mountainous area.

Travelling simulation based on global navigation satellite system accuracy in the orchard

The robot operating system (ROS) was used as the software platform, and Gazebo, an open-source 3D robot simulator with a physics engine, as the simulator. The ROS library, hector_gazebo_plugins, and gazebo_plugins were employed as the virtual module on the simulator. In this simulation, a crawler vehicle was selected as the vehicle model, capable of running on various road surface conditions. Figure 2 shows the crawler vehicle model. Table 3 lists the specifications, control parameters, simulating environment, and sensor modules of the vehicle. The number of sensor modules was set to be as small as possible without compromising the practicality of the farm work. Driving along the target route and detecting workers and obstacles were assumed to be necessary for practical use.

Figure 3 shows the process flow of the control algorithm that adopted the information from the virtual sensor modules. The control algorithm estimated the heading of the vehicle in the direction of travel, and if the vehicle deviated significantly from the target path, it implemented a stop-and-turn manoeuvre on the spot; in other situations, the algorithm implemented feedback control by considering the deviation between the target path and GNSS data. Sonar sensors for the detection of obstacles were mounted in front of each side of the vehicle. If an obstacle was detected on the target path, the vehicle avoided it, and feedback control was resumed when it returned to the path. In the obstacle avoidance mode, the robot moved along the perimeter of the obstacle and aimed to return to the target path. To estimate the vehicle's direction of travel, we applied the Madgwick filter (Madgwick, 2010) to the information obtained from the onboard inertial measurement unit (IMU) and magnetometer to estimate the vehicle's attitude. The point on the target path closest to the GNSS positioning was set as the current point, and that on the target path, 1.5 m from the current point, was set as the reference point. The angle between the line connecting the reference point and GNSS positioning and the vehicle's direction of travel was set as the difference of the yawing angle. If this difference exceeded a threshold, the vehicle was judged to deviate significantly from the route, and the vehicle performed stop-and-turn manoeuvres until the difference was reduced to less than the threshold. The vehicle followed the target path by proportional, integrated, and derivative (PID) control if the difference did not exceed the threshold. Equations 1 and 2 denote the operation value of the right and left crawlers, respectively, and

Table 1. Specifications of the real-time kinematic-global navigation satellite system receiver and stand-alone--global navigation satellite system receiver.

GNSS type	Category	Specifications
RTK-GNSS	Chipset	UBLOX ZWD-F9P Dual frequency support
	Supported satellites system	QZSS (L1, L2) GPS (L1, L2) GLONASS (G1, G2) Galileo (E1, E5) BeiDou (B1, B2)
SA-GNSS	Chipset	MEDIA TEK MT3339 Single frequency support
	Supported satellites system	QZSS (L1) GPS (L1)

GNSS, global navigation satellite system; RTK, real-time kinematic; SA, stand-alone.

Table 2. Experimental conditions in each orchard.

Number of tests [times]	6	5	4
Distance between start and end points [m]	109.66	100.30	45.59
Distance between the start point and first intermediate point [m]	20.57	50.37	26.95
Distance between first and second intermediate points [m]	18.77	0	0
Distance between second intermediate point and end point [m]	70.32	49.93	18.64
This table is written on the north side of the aisle as the starting point			

Equation 3 indicates the system deviation.

$$v_R(t) = \begin{cases} v_{cs}, & e(t) \leq 0 \\ K_p|e(t)| + K_i \int |e(t)|dt + K_d \frac{d|e(t)|}{dt} + v_{cs}, & e(t) > 0 \end{cases} \quad (1)$$

$$v_L(t) = \begin{cases} K_p|e(t)| + K_i \int |e(t)|dt + K_d \frac{d|e(t)|}{dt} + v_{cs}, & e(t) < 0 \\ v_{cs}, & e(t) \geq 0 \end{cases} \quad (2)$$

$$e(t) = e_R(t) - e_L(t) \quad (3)$$

The operating values of the left and right crawlers shown in Equations 1 and 2 are switched by the value of the system deviations shown in Equation 3, respectively. The vehicle can travel following the target path by controlling the operating value according to Equations 1 to 3. In Equations 1-3, K_p, K_i, K_d and v_{cs} denote the proportional control coefficient [–], integral control coefficient [–], derivative control coefficient [–], and value required for constant speed travelling [–], respectively. Furthermore, $e(t)$, $e_R(t)$ and $e_L(t)$ denote the deviations of the control system [–], the difference in the reference point and calculated right crawler position based on GNSS positioning [–], and the difference in the reference point and calculated left crawler position based on GNSS positioning [–], respectively.

The driving environment in the simulation was set to include 50-m-long rows of trees spaced 3.8 m apart. The area of each tree (including the trunk, branches, and leaves) corresponded to a diameter of 0.8 m, based on a simple survey of the actual apple orchard (Figure 4). The road surface conditions in the driving environment in the simulation were assumed to be flat, as the effects of

Figure 1. Photograph of the harvesting route in each field.

Table 3. Specifications, control parameters, and sensor modules of the vehicle.

Category	Item	Value or name
Specifications of vehicle	Mass of body [kg]	22
	Mass of right crawler [kg]	19
	Mass of left crawler [kg]	19
	Full length [m]	0.55
	Full width [m]	0.6
	Full height [m]	0.45
	Width of crawler [m]	0.26
	Length of crawler [m]	0.55
Specifications of Sonar-sensor	Distances of detection possible [m]	0.02-4.00
	Detectable range of vehicle pitching direction [°]	15
	Detectable range of vehicle yawing direction [°]	15
Control parameters	K_p [-]	18
	K_i [-]	5
	K_d [-]	3
	Threshold of yawing angle control [°]	10
Simulating environment	Operating system	Ubuntu 16.04
	Software platform	ROS Kinetic
	Simulator	Gazebo 7.16.0
	Central processing unit (CPU)	Intel Core i7-8700
	Graphics processing unit (GPU)	GeForce GTX1660
Sensor modules	GNSS module (hector-gazebo-plugins)	GazeboRosGps
	Six-axis IMU module (gazebo_ros_pkgs / gazebo_plugins)	gazebo_ros_imu_sensor
	Earth magnetic field sensor module (hector-gazebo-plugins)	GazeboRosMagnetic
	Sonar sensor module (gazebo_ros_pkgs / gazebo_plugins)	gazebo_ros_range

GNSS, global navigation satellite system; IMU, inertial measurement unit.

slippage and other factors are small when only crawler vehicles drive on the road. A position error was added to the GNSS position information in the simulation based on the standard deviation of the actual GNSS measurements in the orchard. The virtual module was mounted on a crawler vehicle, which was assumed to be the actual vehicle, and an orchard driving simulation was conducted. The simulation results were considered to examine the practicality of an orchard robot using GNSS.

Results

Accuracy of real-time kinematic-global navigation satellite system in fruit farms

Figure 5 shows the position information obtained from the RTK-GNSS and SA-GNSS receiver while travelling the same route in the new type of apple field (magnified view of 10 m and 10 m sections in thenorth–south and east–west directions). As shown in Figure 5, the same route can be measured with relatively high accuracy in all the fields when using the RTK-GNSS; however, the SA-GNSS corresponds to a relatively low accuracy in all the fields (Appendix Figures 1-4 show the position information obtained from both receivers while travelling the same route in apple and pear field).

Table 4 lists the mean, maximum, and standard deviation of the misalignment in the lateral direction (perpendicular to the direction of travel) between the approximate lines of each GNSS positioning value in each field. An average discrepancy of approximately 0.15-0.36 m exists between the measurements of the RTK-GNSS in each field. This discrepancy can be attributed to the different positions of the satellites at each measurement instance, the mutual influence of the reception environment, such as foliage and trees blocking the signals, and human error associated with the cart operator. The corresponding discrepancy associated with the GNSS measurements is 1.48-9.43 m, and the misalignment is relatively large in all the fields. The misalignment can likely cause undesirable robot operations, for example, collisions with tree rows while travelling in the orchards.

Figure 6 shows sample positioning plots for the RTK-GNSS receiver during a halt (in the same period) at the midpoint of the new type of apple field. Figure 6 shows that the standard deviations in the north-south and east-west directions for RTK-GNSS are 2.18×10^{-3} m and 3.29×10^{-3} m, respectively. At the same point and time, the standard deviations in the north-south and east-west directions for SA-GNSS are 2.49×10^{-1} m and 1.73×10^{-1} m, respectively (Appendix Figure 5 shows the positioning plots for the SA-GNSS receiver). The positioning data for the distance determination were calculated from the average

values for the GNSS receiver position plots during the halt.

Figure 7 shows the mean and standard deviation of the absolute value of error between the values derived from both GNSS receivers and the actual value in each field. Figure 7 shows that the average error of RTK-GNSS is less than 0.2 m in the short-tree apple field and approximately 0.4 m in the pear and new type of apple field. In addition, the average error of SA-GNSS is 1.8-2.9 m in each field. These results show that the distance travelled by the receiver in the orchard can be estimated with an accuracy of 0.30-0.70 m for RTK-GNSS and 3.0-7.0 m for SA-GNSS. Stable positioning can be realised in each aisle of fields when using RTK-GNSS, and no missing positioning data or erroneous positions that were far from the actual position were observed.

Verification of the effectiveness of real-time kinematic-global navigation satellite system

In the simulation, the vehicle was driven around a row of trees to emulate harvesting operations in the apple field in which this test was conducted. The error of the GNSS module was set to be higher than that for the measured value to ensure a reliable evaluation of the practicality of the robot. In the simulation involving RTK-GNSS, the error deviation from the row central line for each direction (north-south and east-west) was set to have a standard deviation of 1.0 m in amplitude and a mean period of 10 s. The corresponding values for the SA-GNSS were 5.0 m and 10 s. Ten trials were conducted for each type of GNSS to account for the randomness of the error.
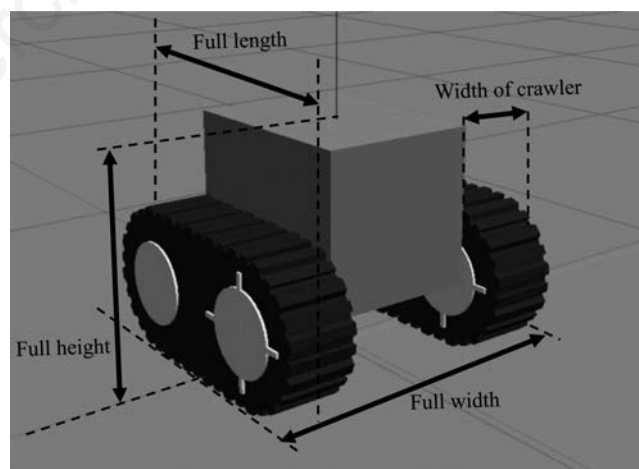

Figure 2. Crawler vehicle model.

Table 4. The mean, maximum, and standard deviation of the misalignment in the lateral direction between the approximate lines of each stand-alone-global navigation satellite system positioning value in each field.

GNSS type	Target field	Average [m]	Maximum value [m]	Standard deviation [m]
RTK-GNSS	Apple field	0.356	0.435	0.127
	New type apple field	0.146	0.215	0.050
	Pear field	0.308	0.648	0.115
SA-GNSS	Apple field	1.479	2.015	0.495
	New type apple field	2.370	3.577	0.792
	Pear field	9.429	16.468	3.633

Figure 8 shows the travelling trajectories for the vehicle equipped with each type of GNSS. The vehicle using RTK-GNSS can travel between the tree rows without collision. However, the vehicle using SA-GNSS significantly deviates from the path after travelling along the sixth row and cannot return to the path. In the 10 trials, the RTK-GNSS vehicle can travel between all rows, but the SA-GNSS vehicle cannot travel along all rows even once. In addition, in one case, the GNSS vehicle overturned because of the significant increase of the control by excessive positioning errors. The mean distances travelled by the RTK-GNSS and SA-GNSS equipped vehicles in each trial are 524.6 m (standard deviation: 0.61 m) and 141.0 m (standard deviation: 91.7 m), respectively. In addition, the average speed in each route is 0.28 ms^{-1} for the RTK-GNSS-equipped vehicles, and the average time of halting per 1 m of travelling is 0.43 s. The corresponding values for the SA-GNSS-equipped vehicles are 0.15 ms^{-1} and 0.78 s. These findings can be explained by the fact that the obstacle avoidance control is activated more frequently in the SA-GNSS-equipped vehicle compared to the RTK-GNSS-equipped vehicle.

Figure 9 shows the mean and standard deviation of the absolute value of the error between the driving trajectory and target path for each GNSS vehicle. The values were calculated from the travelling simulation results of 100 straight, and 90 curved routes for the RTK-GNSS equipped vehicle and 23 straight and 23 curved routes for the SA-GNSS vehicle. Figure 9 shows that the RTK-GNSS-equipped vehicle has an average error of approximately 0.2 m in all routes and travels on the target path more accurately than the GNSS-equipped vehicle. The error of the SA-GNSS-equipped vehicles on all routes is 1.85 times higher than that of the RTK-GNSS-equipped vehicles. However, the error is relatively small for both vehicles on the straight route. This aspect can be attributed to the accuracy of the SA-GNSS and the
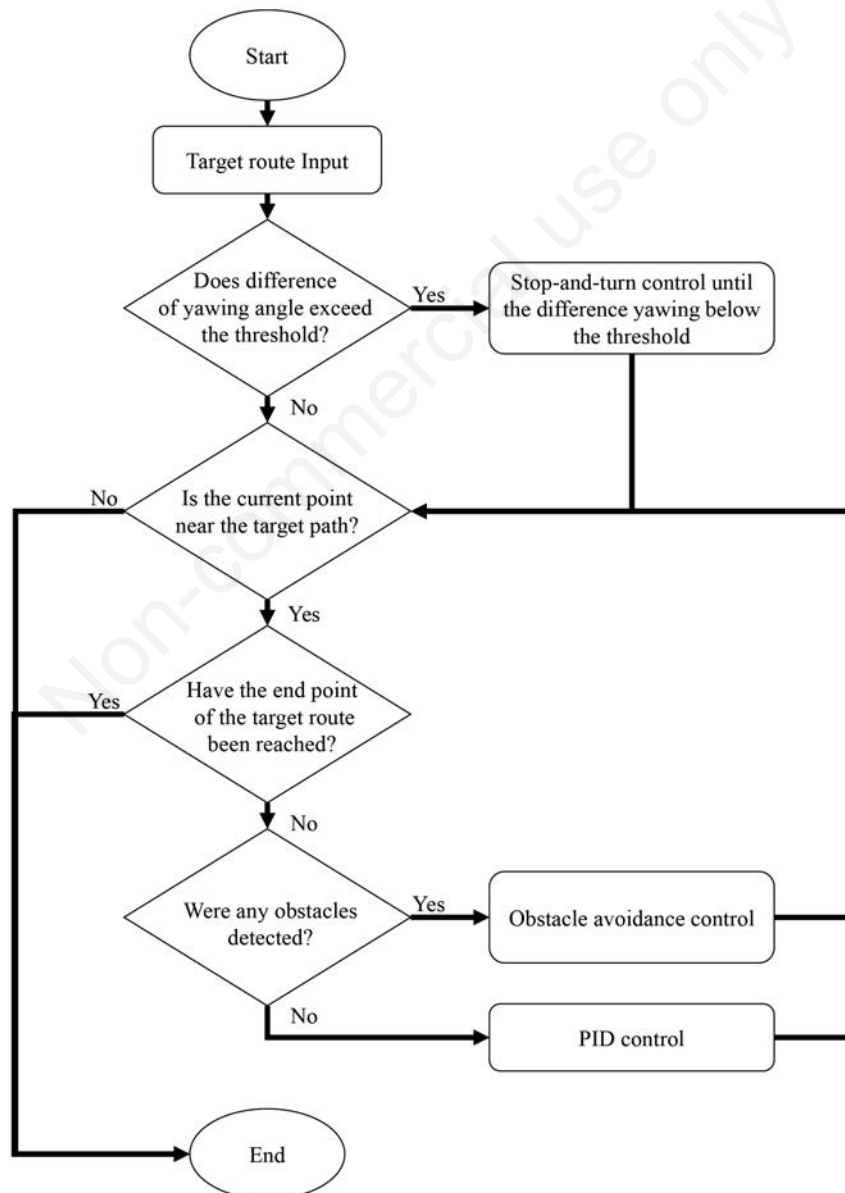

Figure 3. Process flow of the control algorithm.

influence of obstacle avoidance control. The avoidance control effect reduces the maximum error.

In contrast, when driving on a curved route, the error is relatively large for both types of vehicles, with an average error of approximately 0.35 m for the RTK-GNSS-equipped vehicles. The error for the SA-GNSS-equipped vehicles in the case of curved routes is 1.48 times higher than that of RTK-GNSS-equipped vehicles. Therefore, the robot must be prevented from deviating from the path on curved paths when travelling in orchards.

Figure 10 shows the distribution of errors between the target path and traveling trajectory for the RTK-GNSS and SA-GNSS-equipped vehicles. In addition, the percentile of 95% for each clas-
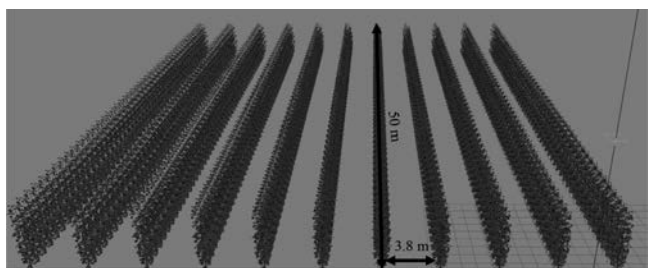
sification of RTK-GNSS are 0.46 m, 0.39 m, and 0.77 m at all driving, straight driving, and cornering driving, respectively. Moreover, the percentile of 95% for each classification of SA-GNSS are 0.66 m, 0.62 m, and 1.23 m at all driving, straight driving, and cornering driving, respectively.

Figure 4. Driving environment in the simulation.

Figure 7. The mean absolute value of error between the value derived from each global navigation satellite system (GNSS) receiver and actual value.
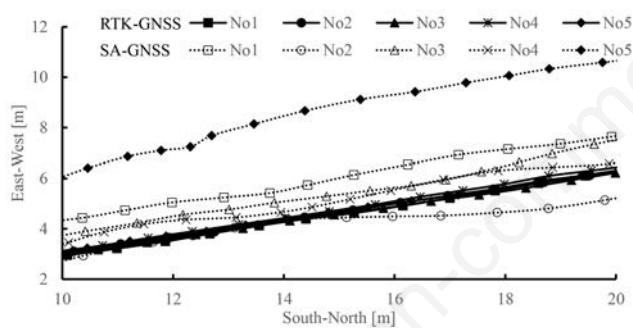

Figure 5. Position information from the real-time kinematic-global navigation satellite system (RTK-GNSS) and stand-alone-GNSS (SA-GNSS) receiver in the new type of apple field.
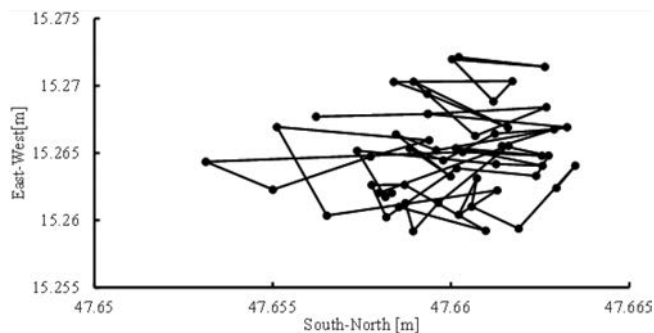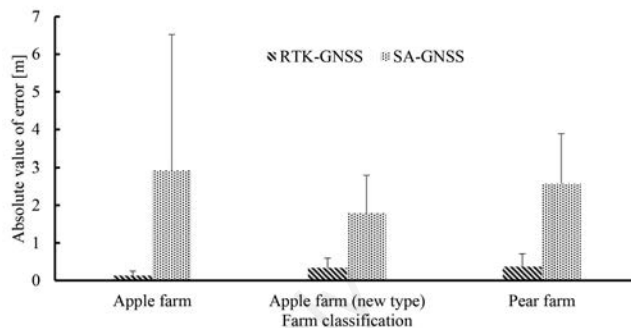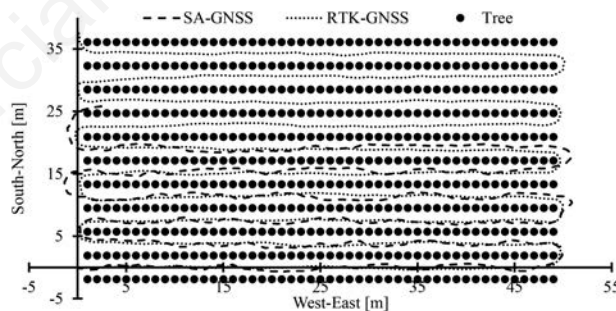

Figure 8. Travelling trajectory for the vehicle using stand-alone-global navigation satellite system (SA-GNSS).

Figure 6. Positioning plots for real-time kinematic-global navigation satellite system (RTK-GNSS) during a halt at the midpoint.
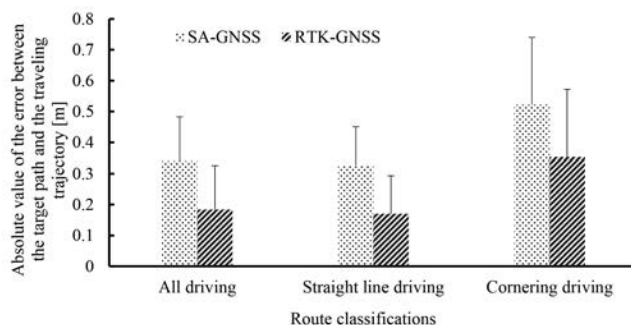

Figure 9. Mean absolute value of error between the driving trajectory and target path for the real-time kinematic-global navigation satellite system (RTK-GNSS) and stand-alone-GNSS (SA-GNSS) equipped vehicles.

OPEN ACCESS

Discussion and Conclusions

The results of both GNSS positioning tests in an orchard near a mountainous area indicate that the RTK-GNSS can attain positioning accuracy with an order of tens of centimetres. The results suggest that RTK-GNSS can be applied to realise practical robotic work in orchards (even near mountainous areas). In addition, the results of simulation with larger GNSS errors based on the actual receiving data show that an agricultural robot equipped with RTK-GNSS and a simple obstacle detection sensor can travel a route with reasonable accuracy even in an orchard near a mountainous area. Moreover, safe driving to prevent collisions with tree rows can be realised by setting the curved route part to have an adequate width. However, the self-positioning accuracy for SA-GNSS-equipped vehicles is low. Notably, the robot cannot drive autonomously in an orchard using only a simple obstacle detection sensor and SA-GNSS, and a sensor is required to enable accurate self-positioning. The proposed method can be used to evaluate the robot's performance having the functions of transporting and harvesting agricultural products in an orchard. In addition, it is possible to examine the robotic operations in other types of orchards by changing the GNSS error size and the position of the trees. Future work can be aimed at examining additional functionalities and different control methods, considering robot operations for orchard environments that can be practically realised at a low cost.

The following conclusions can be derived from this study: i) the results of GNSS positioning tests in an orchard near a mountainous area indicate that in the specific environmental conditions, the RTK-GNSS and SA-GNSS can attain positioning accuracy with an order of tens of centimetres and few metres, respectively; ii) the simulation results based on the GNSS positioning results indicate that a vehicle implementing RTK-GNSS and a simple obstacle detection sensor can travel autonomously in a farmyard without colliding with the tree rows. In contrast, a vehicle implementing SA-GNSS and a simple obstacle detection sensor cannot drive autonomously in an orchard and must realise self-positioning using a more accurate sensor; iii) when driving in an orchard similar to that considered in this study, it is desirable to set a wider route with a margin when setting a target route in a curved section because the error from the target route increases in a curved route; iv) the proposed approach of realising simulations of autonomous agricultural robots based on GNSS data from a real orchard can facilitate the evaluation of practical agricultural robots.
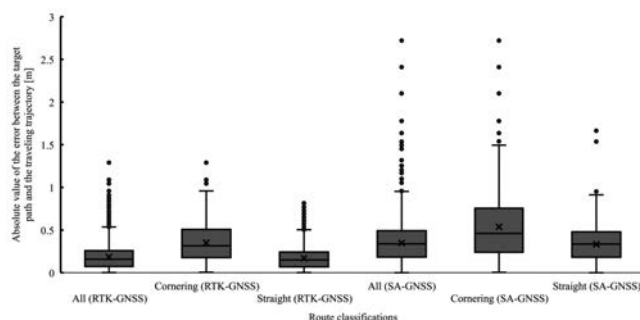

Figure 10. Distribution of errors between target path and travelling trajectory for the real-time kinematic-global navigation satellite system (RTK-GNSS) and stand-alone-GNSS (SA-GNSS) equipped vehicles.

The results demonstrate the possibility of developing small agricultural robots for orchards. We conducted the GNSS positioning test in an orchard at an altitude of approximately 830 m, and similar performance can be expected under similar agricultural situations. Notably, certain agricultural fields in Japan are located in deeper mountainous areas, and GNSS positioning may be difficult in these areas. In addition, in the case of orchards located on sloping terrains, the GNSS self-positioning of vehicles may involve significant errors. Thus, verification using actual autonomous vehicles is necessary, in addition to evaluating robot farming operations such as harvesting and transportation.

Future work

Future work can be aimed at conducting field tests using actual machines. In addition, the developed simulator can be used to evaluate the robot's performance under different environmental conditions, such as slope and road conditions, and under different machine conditions, such as harvesting and transporting functions. For example, if the vehicle hardly travels forward or travels in a direction significantly different from the intended direction due to slipping or getting stuck, simulations that take road surface conditions into account can consider these effects in development. Moreover, GNSS positioning experiments must be conducted in more adverse conditions (disadvantaged agricultural production areas).

References

Allred B, Wishart D, Martinez L, Schomberg H, Mirsky S, Meyers G, Elliott J, Charyton C. 2018. Delineation of agricultural drainage pipe patterns using ground penetrating radar integrated with a real-time kinematic global navigation satellite system. Agriculture 8:11.

Alkan RM, Erol S, İlçi V, Ozulu M. 2020. Comparative analysis of real-time kinematic and PPP techniques in dynamic environment. Measure. J. Int. Measur. Conf. 163:107995.

Barawid Jr CO, Noguchi N. 2008. Automatic guidance system in real-time orchard application (Part 1). J. Japan. Soc. Agric. Machine. 70:76-84.

Barawid Jr CO, Noguchi N. 2010. Automatic guidance system in real-time orchard application (Part 2). J. Japan. Soc. Agric. Machine. 72:243-50.

Blok PM, Boheemen KV, Evert FKV, IJsselmuiden J, Kim GH. 2019. Robot navigation in orchards with localization based on Particle filter and Kalman filter. Comput. Electron. Agric. 157:261-9.

Catania P, Comparetti A, Febo P, Morello G, Orlando S, Roma E, Vallone M. 2020. Positioning accuracy comparison of GNSS receivers used for mapping and guidance of agricultural machines. Agronomy 10:7.

Cheein FA, Steiner G, Paina GP, Carelli R. 2011. Optimized EIF-SLAM algorithm for precision agriculture mapping based on stems detection. Comput. Electron. Agric. 78:195-207.

Chosa T, Omine M, Itani K. 2007. Dynamic performance of global positioning system velocity sensor for extremely accurate positioning. Biosyst. Engine. 97:3-9.

Freeland R, Allred B, Eash N, Martinez L, Wishart D. 2019. Agricultural drainage tile surveying using an unmanned aircraft vehicle paired with real-time kinematic positioning - A case study. Comput. Electron. Agric. 165:104946.

Guevara J, Cheein FAA, Gené-Mola J, Rosell-Polo JR, Gregorio E. 2020. Analyzing and overcoming the effects of GNSS error

on LiDAR based orchard parameters estimation. Comput. Electron. Agric. 170:105255.

Guo J, Li X, Li Z, Hu L, Yang G, Zhao C, Fairbairn D, Watson D, Ge M. 2018. Multi-GNSS precise point positioning for precision agriculture. Precis. Agric. 19:895-911.

Han JH, Park CH, Park YJ, Kwon JH. 2019. Preliminary results of the development of a single-frequency GNSS RTK-based autonomous driving system for a speed sprayer. J. Sens. 2019:9.

Hossein M. 2013. A technical review on navigation systems of agricultural autonomous off-road vehicles. J. Terramechan. 50:211-32.

Iida M, Uchida R, Zhu H, Suguri M, Kurita H, Masuda R. 2013. Path-following control of a head-feeding combine robot. Engine. Agric. Environ. Food 6:61-7.

Japan Ministry of Agriculture. 2020. Forestry and fisheries. A new policy package to accelerate smart agriculture. Available from: https://www.maff.go.jp/j/press/kanbo/kihyo03/attach/pdf/2010 01-1.pdf Accessed: June 24, 2021.

Japan Ministry of Agriculture. 2021. Summary of findings. Forestry and fisheries, 2020 Census of Agriculture and Forestry, Government Statistical Codes: No.00500209,1-10.

Kabir MSN, Song M, Sung N, Chung S, Kim Y, Noguchi N, Hong S. 2016. Performance comparison of single and multi-GNSS receivers under agricultural fields in Korea. Engine. Agric. Environ. Food 9:27-35.

Kaizu Y, Tsutsumi T, Igarashi S, Imou K. 2018. Development of autonomous driving control system for a robot mower using a low-cost single-frequency GNSS and a low-cost IMU. J. Japan. Soc. Agric. Machine. Food Engine. 80:271-9.

Kawase K. 2011. A more concise method of calculation for the coordinate conversion between geographic and plane rectangular coordinates on the Gauss-Kruger projection. J. Geospat. Inf. Author. Japan 109-24.

Kayacan E, Kayacan E, Ramon H, Saeys W. 2014. Nonlinear modeling and identification of an autonomous tractor-trailer system. Comput. Electron. Agric. 106:1-10.

Keicher R, Seufert H. 2000. Automatic guidance for agricultural vehicles in Europe. Comput. Electron. Agric. 25:169-94.

Kise M, Noguchi N, Ishii K, Terao H. 2002. Field mobile robot navigated by RTK-GPS and FOG (Part 3). J. Japan. Soc. Agric. Machine. 64:102-10.

Li M, Imou K, Wakabayashi K, Ykoyama S. 2009. Review of research on agricultural vehicle autonomous guidance. Int. J. Agric. Biol. Engine. 2:1-16.

Madgwick OHS. 2010. An efficient orientation filter for inertial and inertial/magnetic sensor arrays. Report x-io and University of Bristol (UK), 25:113-118.

Matsuo Y, Yukumoto O, Yamamoto S, Noguchi N, Hara Y. 2009.

Improvement of adaptability and reliability of tilling robot (Part 3). J. Japan. Soc. Agric. Machine. 71:85-93.

Miyamoto J, Naomoto T, Kubota Y, Yoshida K, Ishimi K. 2017. Rice transplanter with straight keeping system. The Proceedings of Conference of Kansai Branch 2017:92-301.

Nagasaka Y, Taniwaki K, Otani R, Shigeta K, Sasaki Y. 2000. The development of autonomous rice transplanter (Part 1). J. Japan. Soc. Agric. Machine. 61:179-86.

National Agriculture and Food Research Organization. 2019. The number of deaths per 100,000 workers over 10 years. Available from: http://www.naro.affrc.go.jp/org/brain/anzenweb/shi-bou/pdf/20210216press-ref.pdf Accessed: June 24, 2021.

Nagano Prefecture. 2020. Overview of the governor's special area for direct agricultural payment scheme in mountainous areas. Available from: https://www.pref.nagano.lg.jp/noson/nosonshinko/docu-ments/siryou2tokuningaiyou.pdf Accessed: June 24, 2021.

Nørremark M, Griepentrog HW, Nielsen J, Søgaard HT. 2008. The development and assessment of the accuracy of an autonomous GPS-based system for intra-row mechanical weed control in row crops. Biosyst. Engine. 101:396-410.

Ogura Y. 2017. John Deere's auto trac technology for agriculture vehicle. J. Japan. Soc. Agric. Machine. Food Engine. 71:85-93.

Pérez-Ruiz M, Carballido J, Agüera J, Gil JA. 2011. Assessing GNSS correction signals for assisted guidance systems in agricultural vehicles. Precis. Agric. 12:639-52.

Pérez-Ruiz M, Martínez-Guanter J, Upadhyaya KS. 2021. Chapter 15 - High-precision GNSS for agricultural operations. GPS GNSS Technol. Geosci. 299-335.

Pini M, Marucco G, Falco G, Nicola M, Wilde WD. 2020. Experimental testbed and methodology for the assessment of RTK GNSS receivers used in precision agriculture. IEEE Access 8:14690-703.

Rovira-Más F, Chatterjee I, Sáiz-Rubio V. 2015. The role of GNSS in the navigation strategies of cost-effective agricultural robots. Comput. Electron. Agric. 112:172-83.

Santos AF, Silva RP, Zerbato C, Menezes PC, Kazama EH, Paixão CSS, Voltarelli MA. 2019. Use of real-time extend GNSS for planting and inverting peanuts. Precis. Agric. 20:840-56.

Søgaard HT, Lund I. 2000. Application accuracy of a machine vision-controlled robotic micro-dosing system. Biosyst. Engine. 96:315-22.

Weise G, Nagasaka Y, Taniwaki K. 2000. Research note (PM-power and machinery): an investigation of the turning behaviour of an autonomous rice transplanter. J. Agric. Engine. Res. 77:233-7.

Zhang Z, Noguchi N, Ishii K. 2015. Development of a robot combine harvester. J. Japan. Soc. Agric. Machine. Food Engine. 77:45-50.